We are IntechOpen,
the world's leading publisher of Open Access books
Built by scientists, for scientists

4,800
Open access books available

122,000
International authors and editors

135M
Downloads

Our authors are among the

154
Countries delivered to

TOP 1%
most cited scientists

12.2%
Contributors from top 500 universities

CLARIVATE ANALYTICS
BOOK CITATION INDEX
INDEXED

WEB OF SCIENCE™

Selection of our books indexed in the Book Citation Index
in Web of Science™ Core Collection (BKCI)

Interested in publishing with us?
Contact book.department@intechopen.com

Numbers displayed above are based on latest data collected.
For more information visit www.intechopen.com

Integrated Biomimemic Carbon Nanotube Composites for Biomedical Applications

L. Syam Sundar, Ranjit Hawaldar, Elby Titus,
Jose Gracio and Manoj Kumar Singh

Additional information is available at the end of the chapter

1. Introduction

In recent years Nanotechnology form a fascinating interdisciplinary area that brings together biology, material science, and nanoelectronics. Moreover, mainly three different applications of nanotechnology particularly suited to biomedicine: diagnostic techniques, drugs, and prostheses and implants. Interest is booming in biomedical applications for use outside the body, such as diagnostic sensors and "labon- a-chip" techniques, which are suitable for analyzing blood and other samples, and for inclusion in analytical instruments for R&D on new drugs. For inside the body, many companies are developing nanotechnology applications for anticancer drugs, implanted insulin pumps, and gene therapy. Nanotechnology also has applications in the tissue engineering field, helping people who are in need of new bones, teeth, or other body tissues by replacing damaged or missing tissue with an equivalent material. The biological material is introduced into a mould to produce a body part with a characteristic shape, a bone for example. There is a long list of these devices such as orthopedic joint prostheses cardio vascular aids and dental implants; however the theme prepared aims only the first one; orthopedic joint prostheses, with particular emphasis on hip and knee ortheoplasty. Survival of the arthroplasty depends among others on the age of the patient. In patients over 65, failure rate after ten years is about 7 %. In younger patients (<60 year) failure rates are significantly higher (>15%). As the number of arthroplasties will grow due to the ageing of our population, a considerable percentage of this increase will consist of revision arthroplasties. Because results of revisions are worse than those of primary arthoplasties, improved procedures for placement of joint prostheses have to be found. Therefore, an implant made of a mechanically strong material that can support and even enhance the integration of orthopedic implants will increase the clinical effectiveness of bone implants and will make it less likely that the implants will wear out and need to be replaced. The worldwide

emergence of nano scale science and engineering will make viable the production of enhanced biomaterials with high compatibility of interacting with the human biological systems.

Of significant biological importance when utilizing this technology is to exercise control over mechanical properties at the material-biological interface (Discher et al., 2005). Manipulation of mechanical properties within these systems can dictate cell response and affect many physiological responses (LeDuc and Robinson, 2007; LeDuc and Bellin, 2006). CNTs have already been employed in the mechanics of materials domain for decades because of their high strength, which makes them ideal for a variety of applications including polymeric composite systems. Their successes *in vivo* though have been inhibited by physiological challenges as the promise of introducing pristine nonfunctionalized CNTs in polymer matrixes has been limited because this type of nanomaterial is practically insoluble and can accumulate in cells, organs, and tissues with dangerous effects (Zanello et al., 2006; Lam et al., 2004). This problem has been overcome, however, by chemically modifying the surfaces of the CNTs, which addresses the solubility challenges in most solvents and polymers (Colvin, 2003; Ajayan and Tour, 2007; Coleman et al., 2006).

However, current joint implants last only 10 to 15 years before failing. Because of this, many patients have to go through a revision surgery due to the failure of bone implants. The main reason for implant failure is aseptic loosening of the implant from juxtaposed bone. In this light, polymethyl methacrylate (PMMA) has been used widely in orthopedics to improve the bonding between the implant and bone. In total hip replacement procedures, PMMA cement is located at the bone-implant interface and plays an important role in inhibiting the aseptic loosening processes. PMMA cement is associated with several drawbacks that limit its efficacy (such as strong exothermic reactions, weak radiopacity and poor fatigue strength; all leading to insufficient bonding to bone). With an expectation of increased revision surgeries and patients receiving orthopaedic implants in the coming years, the emphasis of joint replacement research needs to be focused on improving the mechanical and biocompatibility properties of bone cements. As nanotechnology has been extensively used to improve mechanical and surface properties of implant materials, it certainly provides a unique opportunity to modify the material properties of currently used bone cements in a more precise manner.

For developing a biologically inspired composite system, there are numerous available composite materials. One particular area that has shown promise is in using bone cements such as PMMA. PMMA has been extensively used in orthopaedic surgery as a biomaterial that fixes artificial joints to bone and fills bone defects, as well as a drug-delivery system (Rimessi et al., 2009). One well documented issue with bone cements is that the fixation strength of PMMA cement to bone is primarily dependent on mechanical characteristics. To address this, a complementary material, hydroxyapatite (HA) (Singh et al., 2008), has been used with PMMA. HA is a prime constituent of bone cements and is particularly useful for a diversity of reasons including its ability to bond chemically with living bone tissues as well as its chemical and crystalline similarity to human skeletal apatite. These systems alone

though exhibit intrinsic brittleness and poor strength, thus restricting its clinical applications under load-bearing conditions (Curtin and Sheldon, 2004; Vallo et al., 2004; McGee et al., 2000; Stevens, 2008).

In the present chapter we will review the previous bone cements, future prospects and application of carbon nanotubes based nanocomposites for the development of next generation active bone cement for biomedical applications, which have been particularly relevant in our research group at TEMA.

2. Polymethylmethacrylate (PMMA) or bone cement

Polymethylmethacrylate (PMMA), a clear plastic, is a pretty versatile material. Plexiglas windows are made from PMMA. Acrylic paints contain PMMA. It also remains one of the most enduring materials in orthopedic surgery where it has a central role in the success of total joint replacement. Being part of a group of medical materials called 'bone cement', its use includes the fixation of biomaterials such as artificial joints to bone, the filling of bone defects and, also, as a drug-delivery system. Beginning in the 1970s, many successful results have been reported for total hip replacement using PMMA cement; however, failures of fixation have also occurred. The fixation strength of PMMA cement to bone is mainly dependent on mechanical interlocking, but it is known that a fibrous tissue layer intervenes between cement and bone - PMMA cement never bonds directly to the bone. One of the problems associated with the conventional types of bone cement used is their unsatisfactory mechanical and exothermic reaction properties. Other problems with PMMA cement include the biological response, leakage of the monomer of methylmethacrylate and a high curing temperature, which can damage cell activity. Ideally, a bone cement material must functionally match the mechanical behavior of the tissue to be replaced, it must be able to form a stable interface with the surrounding natural tissue and be effective in guided tissue regenerative procedures, it should be easy to handle, biologically compatible, non-supporting of microbial growth, and non-allergenic.

3. Hydroxyapatite (HA)

Hydroxyapatite (HA) is another key constituent of bone cements because of its ability to bond chemically with living bone tissues; this is due to its similar chemical composition and crystal structure to apatite in the human skeletal system. However, the intrinsic brittleness and poor strength of sintered HA restricts its clinical applications under load-bearing conditions.

4. Carbon nanotubes

Carbon nanotubes (CNTs) are allotropes of carbon with a cylindrical nanostructure. Nanotubes have been constructed with length-to-diameter ratio of up to 132,000,000:1 (Dai, 2002) significantly larger than for any other material. These cylindrical carbon molecules

have unusual properties, which are valuable for nanotechnology, electronics, optics and other fields of materials science and technology.

Carbon nanotubes are the strongest and stiffest materials yet discovered in terms of tensile strength and elastic modulus respectively. This strength results from the covalent sp^2 bonds formed between the individual carbon atoms. In 2000, a multi-walled carbon nanotube was tested to have a tensile strength of 63 giga pascals (Gpa) (Yu et al., 2000). Further studies, conducted in 2008, revealed that individual CNT shells have strengths of up to ~100 GPa, which is in good agreement with quantum/atomistic models (Peng et al., 2008). Since carbon nanotubes have a low density for a solid of 1.3 to 1.4 g/cm^3 (Collins, 2000) its specific strength of up to 48,000 kN-m/kg is the best of known materials, compared to high-carbon steel's 154 kN-m/kg. Standard single-walled carbon nanotubes can withstand a pressure up to 24 GPa without deformation. They then undergo a transformation to super hard phase nanotubes. Maximum pressures measured using current experimental techniques are around 55GPa. The bulk modulus of superhard phase nanotubes is 462 to 546 GPa, even higher than that of diamond (420) GPa for single diamond crystal) (Popov, 2003).

4.1. Dispersion of functionalized carbon nanotubes in the water

Commercially available (purity >95%, Nanocyl-3150) multi-walled carbon nanotubes with lengths of 1-5 μm and diameters of 5-10 nm were suspended in 3:1 mixture of concentrated H_2SO_4 (18.4 M)/HNO_3(16M) and sonicated in a water bath for 24 hours. The resulting suspension was then diluted with water, and the MWCNTs were collected on a 100-nm-pore membrane filter and washed with deionized water. The resultant functionalized MWCNTs (MWCNTs-COOH) were investigated by FTIR (Nicolet AVATAR-360 FT-IR spectrophotometer) and visible micro-Raman spectra (Jobyin Ivon T64000, λ=514.5 nm). IR spectra of COOH functionalized MWCNTs shows carbonyl stretching at 1729 cm^{-1} but in Raman spectra this signal is inactive. In Raman spectra a band centred at 1300 cm^{-1} is attributed to sp^3-hybridized carbon in the hexagonal framework of the nanotube walls. This disorder mode band is enhanced, as functional groups are attached to the side walls of the nanotubes (Ying et al., 2003; Dyke and Tour, 2003; Georgakilas et al., 2002; Dyke and Tour, 204; Wang and Tseng, 2007). Acid-base titrations (Zho and Stoddart, 2009; Tsang et al., 1994) were performed to determine the concentration of COOH groups for acid-treated MWCNTs. The result indicates that around 3% Carbon atoms are functionalized with COOH groups.

To obtain a homogeneous dispersion of MWCNTs-COOH in water, it was used an aqueous dispersant "NanoSperse AQ" (http://www.nano-lab.com/dispersant-suspensions.html) a surfactant, which consists mainly of poly (oxy-1,2-ethanediyl), tertramethyl-5-decyne-4,7-diol and butoxyethanol, respectively. The typical procedure involves mixing of 100 mg of MWCNTs-COOH in 100 ml of distilled water with 4 ml of dispersant, and then keeping the mixture in a ultrasonication bath for one hour. The final product presents a black colour with no settling of MWCNTs (Figure 1).
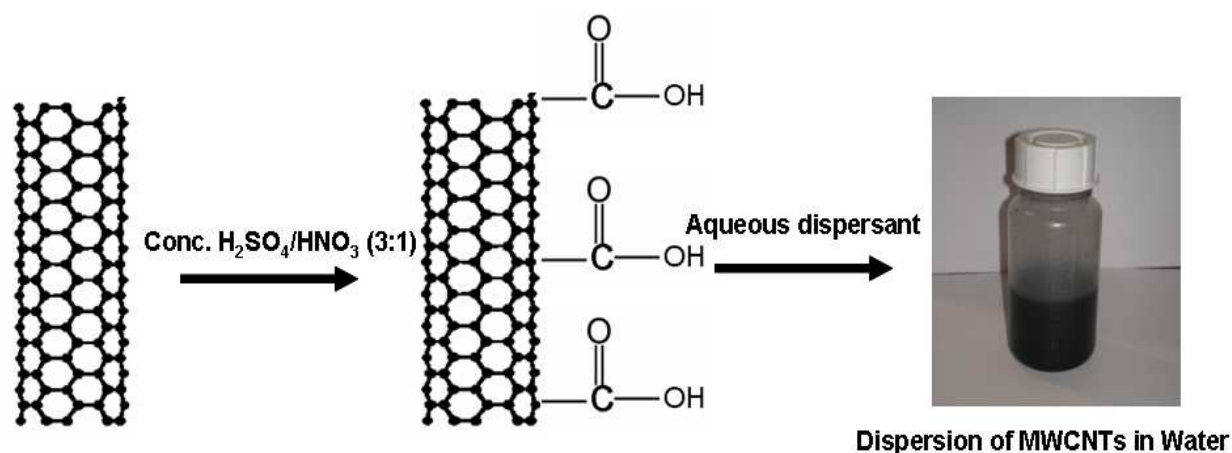
Figure 1. Schematic diagram for chemical fictionalization of MWCNTs and their dispersion in water

5. Carbon nanotube-reinforced poly (methyl methacrylate) nanocomposite for bone cement application

Carbon nanotubes, due to their small dimensions and high aspect ratio, exhibit exceptional physical and chemical properties (Iijima, 1991; Baughman et al., 2002; Usui et al., 2008). No other material can compete with their outstanding combination of mechanical, thermal and electronic properties, which makes them an outstanding reinforcement material for composites (Goller et al., 2003; Cholpek et al., 2006; Price et al., 2003; Peigney, 2003). The ideal reinforcement material would impart mechanical integrity to the composite at high loadings, without diminishing its bioactivity. Hydroxyapatite (HA) is the prime constituent of bone cements, because of its ability to bond chemically with living bone tissues due to its similar chemical composition and crystal structure to apatite in the human skeletal system. However, the intrinsic brittleness and poor strength of sintered HA restricts its clinical applications under load-bearing conditions (Dimitrievska et al., 2008; White and Best, 2007). The polymethyl methacrylate is another material commonly used as bone cement; however, its low mechanical strength makes the use of PMMA problematic. In the present work, a novel nanocomposite material was synthesized comprising MWCNTs, PMMA and HA, which promises to be a superior material for biomedical applications. The selection of PMMA was made for two main reasons: (i) PMMA is already used as bone cement, and it is highly compatible with HA, and (ii) MWCNTs are highly stable in its original form and PMMA can act as a functionalizing and linking material with HA.

There are two main goals when preparing the MWCNTs/PMMA/HA nanocomposite, namely: (i) to obtain homogenous dispersion of the MWCNTs, ensuring uniform properties throughout the composite, and (ii) to enhance the interaction between the MWCNTs and mixing material to achieve an appropriate level of interfacial stress transfer. The dispersion of the MWCNTs is probably the most pressing issue. The MWCNTs should be uniformly dispersed to guarantee that they are individually coated with PMMA-modified HA composite, which is imperative in order to have an efficient load transfer to the MWCNTs network. This also results in a more uniform stress distribution and minimizes the presence

of loci of high stress concentration. To this purpose the percentage of MWCNTs in the nanocomposite material should be controlled – a large amount of MWCNTs cause them to bundle up in weakly interacting tubes as a result of the van der Waals attraction (Kis et al., 2004), and, moreover, it will decrease the interfacial interaction between the mixing material and the MWCNTs.

5.1. Freeze-granulation technique to produce the nanocomposite of PMMA and HA with dispersed MWCNTs

The well dispersed MWCNTs mixture in water was obtained for four different weight percentages of MWCNTs, namely 0.01%, 0.1%, 0.5% and 1% MWCNTs, respectively. Each solution was mixed with a composite of commercially available PMMA (high viscosity bone cement purity >99%, Johnson and Johnson Co.) and HA (particle size 2-3 μm with purity >98%, Agoramat-Advanced Materials) in 1:2 weight percentage. The homogenous mixture of HA powders and PMMA were prepared by ball-milling (Satish Kumar et al., 1996; Tsang et al., 1994; Chen et al., 2005; Walker et al., 2007; Poudyal et al., 2004). There is no effect on HA powder size distribution during ball milling it restricts agglomeration of HA powder during mixing of PMMA with HA.

The *freeze-granulation technique* (Power Pro Freeze-granulator L5-2, Sweden)   was performed with the objective of drying the nanocomposite of MWCNTs-reinforced PMMA/HA powder to preserve the material homogeneity and enhance the dispersion of the nanoparticles in the composite matrix. Figure 2 shows the schematic diagram for the step-by-step procedure, which yields the synthesis of MWCNTs-reinforced PMMA/HA nanocomposite using the *freeze-granulation technique*. Granules with no cavities can be performed and no migration of small particles will give a high degree of granule homogeneity, while mild drying avoids oxidation of the powder. Also, lower granule density and the aid of evenly distributed low concentration MWCNTs will give softer granules with a wide granule size distribution. The freeze dried nano-particles were then collected and finally dried in vacuum for 3 days. In order to dry any remaining liquid the nano-composite was kept for 24 hours in the oven set at 40°C.

5.2. Surface characterization and mechanical properties

Field-Emission Scanning Electron Microscopy (Hitachi S-800, and SU-70, 30 keV) was performed to study the dispersion and distribution of the MWCNTs in PMMA modified HA matrix. The phase composition and purity of the samples were investigated by using the Philips Xpert-MPD X-ray powder diffractometer with Co Kα radiation at 45 kV and 40 mA. Room temperature micro-Raman studies were also performed to study the integration of MWCNTs with the PMMA-HA nanocomposite material. Figures 3-6 show the surface morphology of the MWCNTs-reinforced samples for 0.00%, 0.01%, 0.1% and 1.0% of MWCNTs, respectively. From the SEM observations for different concentrations of MWCNTs reinforced samples, it is clearly observed the concentration of 0.1% of MWCNTs yields the best reinforcement for the PMMA/HA nanocomposite (Figures 5 a,b). For 0.1%
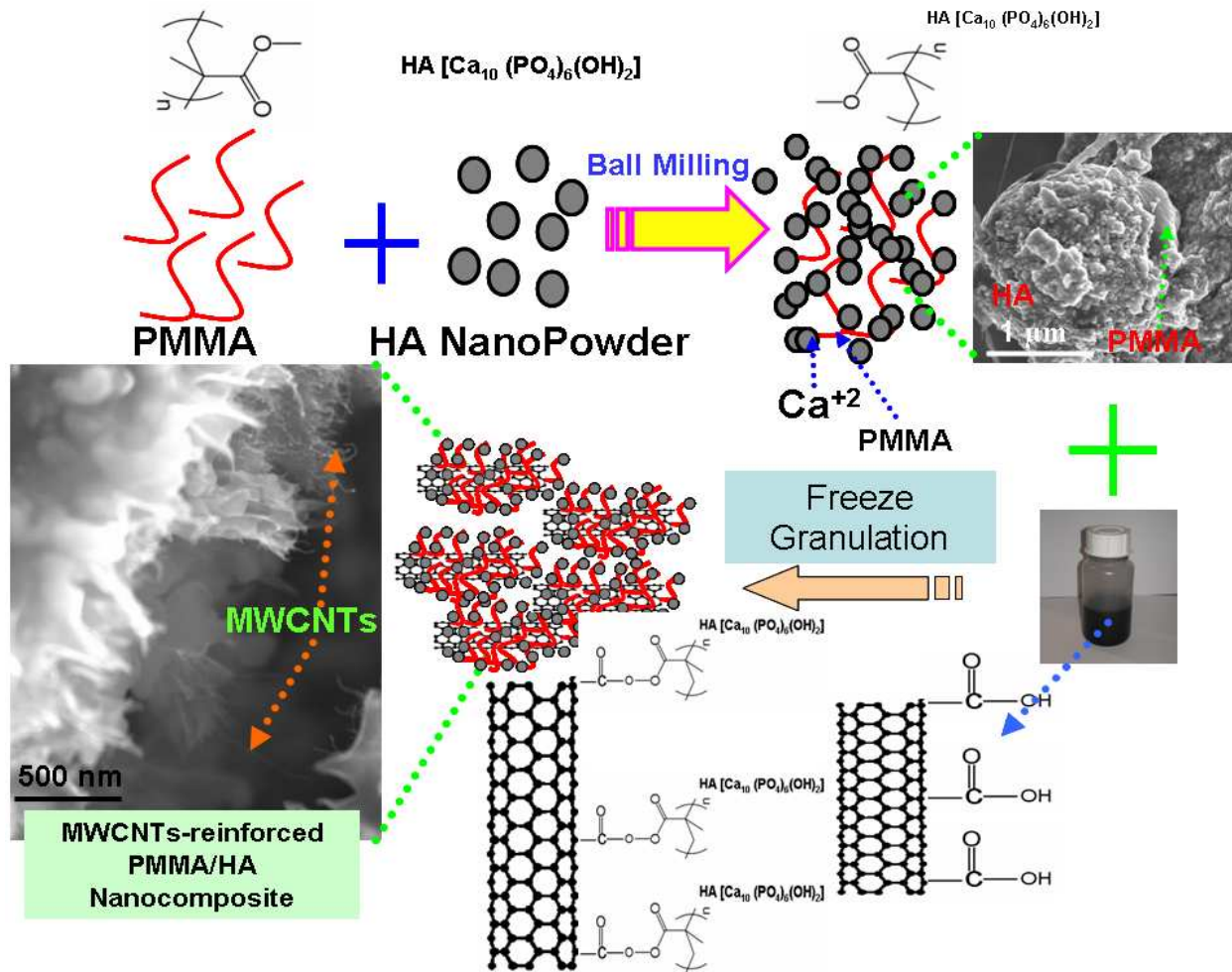
Figure 2. Schematic diagram for the formation of MWCNTs-reinforced PMMA/HA nanocomposite by the freeze-granulation technique

oncentration of MWCNTs, an intercalation of the PMMA/HA composite inside the MWCNTs distribution does occur (Figures 6 a,b), leading to an increase in the MWCNTs dispersion. Below this concentration, the mutual interaction between two adjacent MWCNTs is practically non-existent, which tends to decreases the homogeneity of the nanotubes inside the PMMA/HA matrix. Figure 2 depicts the surface morphology of the 0.01% MWCNTs -PMMA/HA nanocomposite. At higher nanotube concentrations, because less PMMA/HA is available to intercalate into the MWCNTs distribution may lead to weak bonding between the PMMA/HA and MWCNTs, making the composite weak in strength. The SEM image of 1% MWCNTs -PMMA/HA composite shows agglomeration of MWCNTs into bundles. This indicates that the PMMA/HA did not intercalate into the bundles. Only the outside nanotubes of a bundle can be bonded to the composite (Figure 5.6).
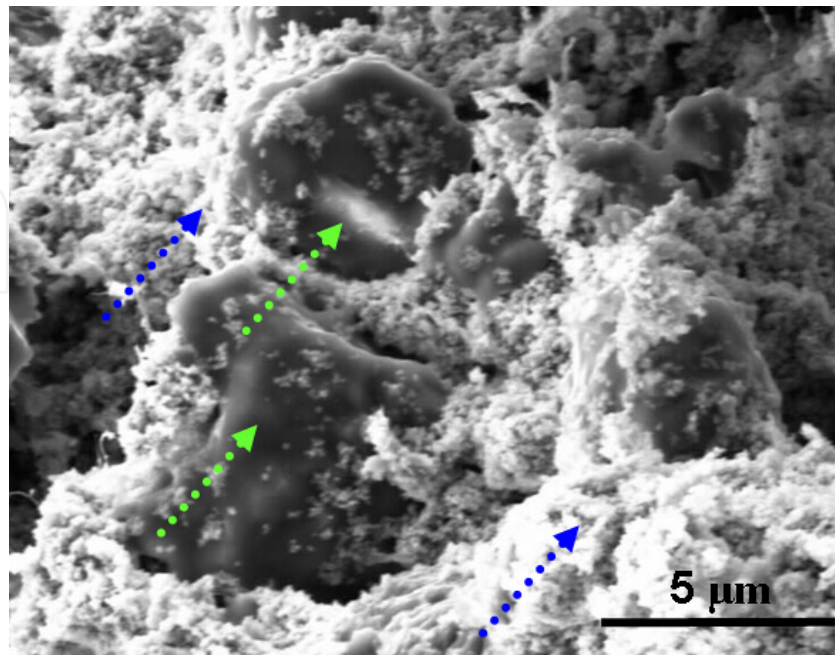
Figure 3. FE-SEM image showing the surface morphology of 0.00% MWCNTs-PMMA/HA nanocomposite, prepared by ball milling. The blue and green dotted arrows indicate HA and PMMA phases in the PMMA/HA composite.
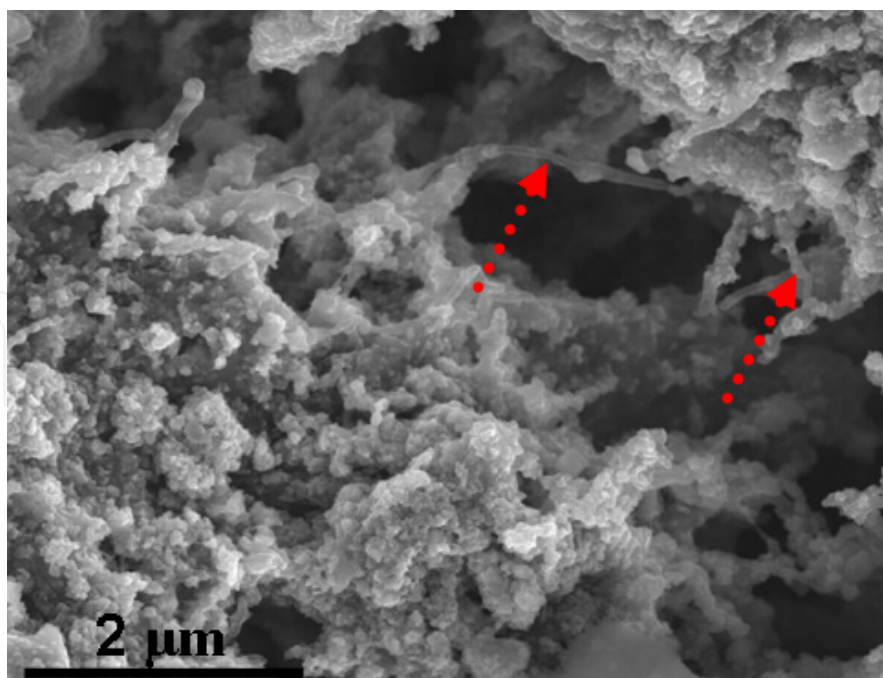

Figure 4. FE-SEM image showing the surface morphology for 0.01% MWCNTs -PMMA/HA nanocomposite, prepared by *freeze-granulation technique*. From this image (indicated by a red dotted arrow), it can be observed that some MWCNTs sheathed with the PMMA/HA nanocomposite.
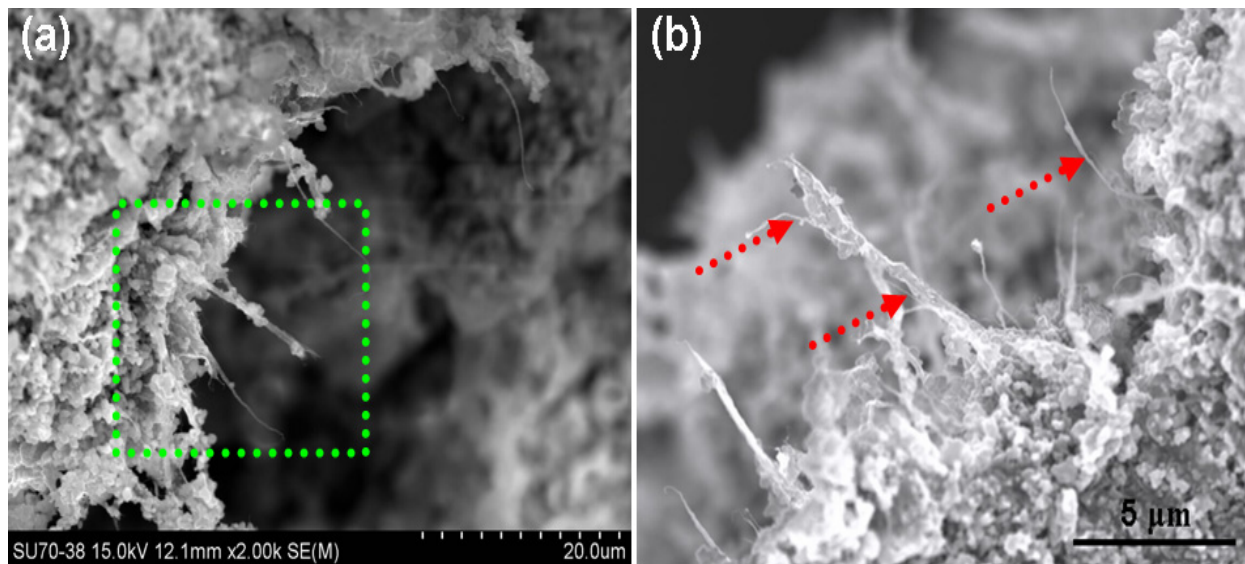
Figure 5. (a) FE-SEM image showing the surface morphology of 0.1% MWCNTs-PMMA/HA nanocomposite. (b) Shows the highly magnified SEM image of the area denoted by a green dotted square in (a) and the red dotted arrows point to isolated MWCNTs, which are completely covered by the PMMA/HA matrix.
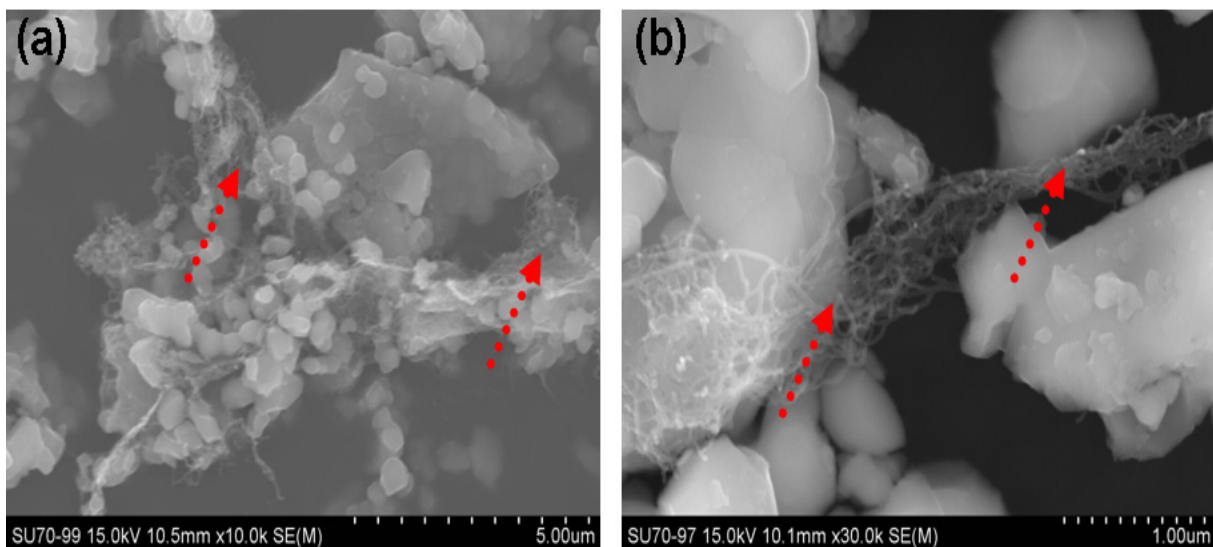

Figure 6. (a,b) FE-SEM images performed at various locations of the 1% MWCNTs -PMMA/HA composite sample shows agglomeration of MWCNTs networks (denoted by the red dotted arrows). This indicates that PMMA/HA did not intercalate into the networks; therefore, only the outside nanotubes of a network can bind to the composite.

Figure 7 illustrates the X-ray diffraction (XRD) patterns of PMMA, HA and 0.1% MWCNTs-PMMA/HA, respectively. It is clearly shown the main constituent phases of the composite are crystalline HA (Haque et al., 2007; Bouyer et al., 2000) (JCPDS 09-0432). No MWCNTs peaks were found in the XRD pattern of the 0.1% MWCNTs-PMMA/HA composite, most likely because for small percentages of MWCNTs detection is not possible within the sensitivity limit of XRD. Miller indices of the diffraction peaks are given in parentheses. PMMA, which is an amorphous polymer (Meneghetti et al., 2004), shows a broad peak at 2θ

value of 13°. The shape of the most intense broad peak reflects the ordered packing of polymer chains (Ryu et al., 2004).
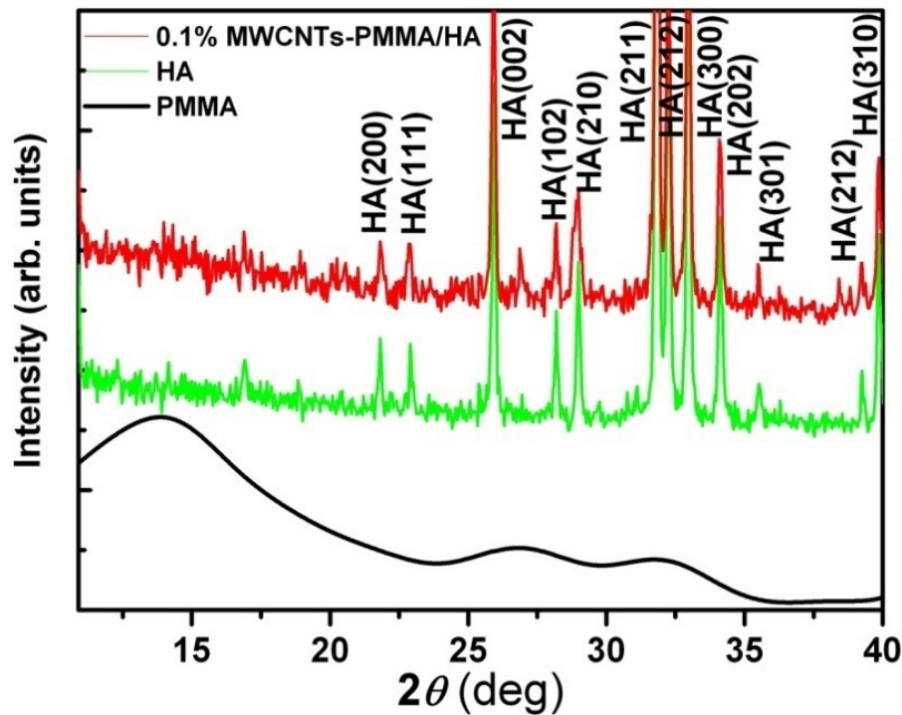

Figure 7. XRD results of PMMA, HA and 0.1% MWCNTs-PMMA/HA, respectively, in the composite. PMMA presents a broad amorphous peak at 2θ value of 13°.
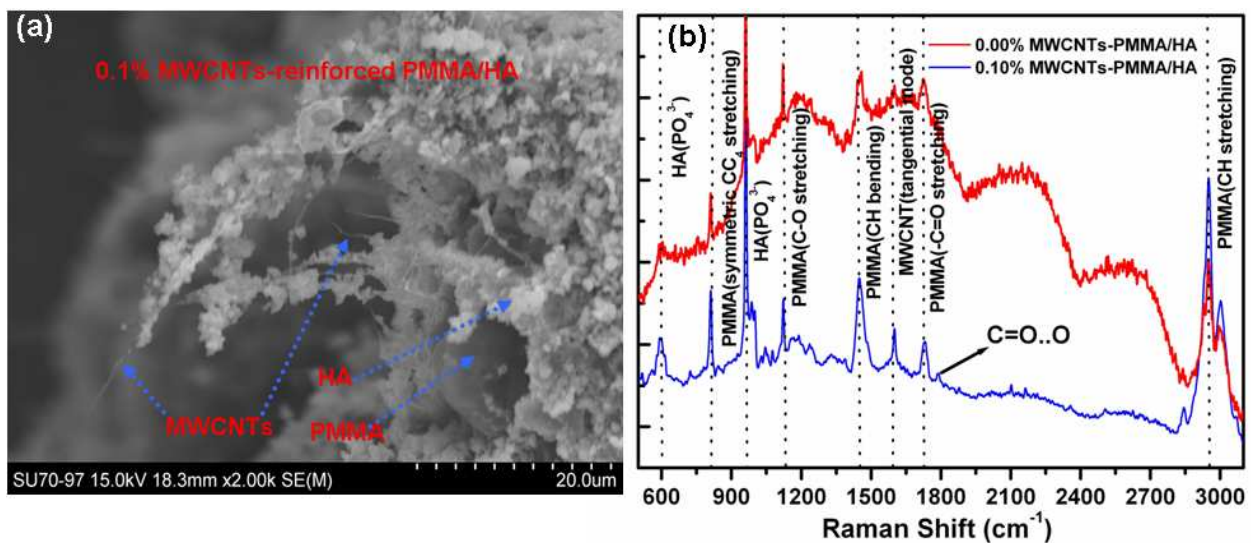

Figure 8. (a) FE-SEM image of 0.1% MWCNTs-reinforced PMMA/HA sample prepared by *freeze-granulation technique* (b) Raman spectra (denoted by the blue line) collected from a 0.1% MWCNTs-reinforced PMMA/HA sample shown in (a).

The visible Raman spectra collected from the 0.1% MWCNTs-reinforced PMMA/HA sample (Figure 8a) denoted by a blue line in Figure 8b, shows several distinct features. The feature near 1773 cm^{-1} is attributed to C=O. O bonded and indicates that COO$^-$ functional groups in

functionalized MWCNTs interact with C=O of PMMA (Velasco-Santos et al., 2003; Velasco-Santos et al. 2002; Hong et al., 2002). Also, it can be observed several other peaks at 602 (PO_4^{3-}), 962 (PO_4^{3-}), 1592 (tangential mode) and 814 (symmetric CC_4 stretching), 1452 (CH bending), 1123 (C-O stretching), 1724 (-C=O stretching), 2952 (CH stretching) cm^{-1} which are due to the HA, MWCNTs and PMMA, respectively (Paillet et al., 2004; de Mul et al., 1986; Suzuki et al., 1991; Kim et al., 2004; Matsushite et al., 2000).

Nanoindentation tests were performed using a MTS Nano Indenter XP with a Berkovich diamond tip. Hardness and elastic modulus of the PMMA/HA nano-composite with different percentage of MWCNTs were measured as a function of the indentation depth using a continuous stiffness measurement (CSM) method. The typical nanoindentation test consists of seven subsequent steps: approaching the nanocomposite surface; determining the contact point; loading to peak load; holding the tip for 10 s at the peak load; unloading 90% of peak load; holding the tip for 100 s at 10% of the peak load for thermal drift correction; and finally, unloading completely. The hardness and elastic modulus were obtained from the curves using the Oliver-Pharr method (Suzuki et al. 1991).

In the present work the nanoidentation technique is employed to study the variation of the mechanical properties of MWCNTs-reinforced PMMA/HA composite with different concentrations of MWCNTs. Figure 9 displays the typical load-displacement curves at a peak indentation load of 10 mN on the MWCNTs-reinforced PMMA/HA composite; it clearly demonstrates that no cracks were formed during indentation. A considerable amount of creep strain at the peak load was found for all the samples. The holding segment at the peak load is necessary for the dissipation of creep displacement; most polymeric biomaterials and tissues often exhibit this type of time-dependent or viscoelastic behaviour (Li and Bhushan, 2002; Bhushan, 2003).
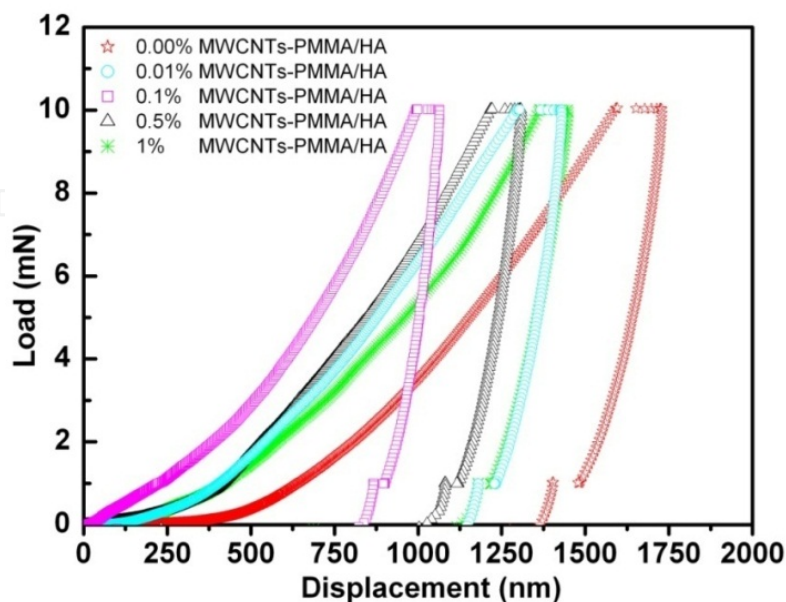

Figure 9. Typical load-displacement curves of indentations made at a peak indentation load of 10 mN on the PMMA/HA nanocomposite and its MWCNTs-reinforced samples.

To study the effect of dispersion of nanotubes in the PMMA/HA composite, hardness and elastic modulus values are needed for both small and large indentation depths. Thirty two nanoindentation tests were carried out on each sample, and the experimental errors are ±0.60 GPa for the elastic modulus and ±0.05 GPa for the hardness. The hardness and elastic modulus values as a function of the indentation depth for PMMA/HA and its MWCNTs reinforced samples are presented in Figure 10 and the average hardness and elastic modulus for these composites are listed in Table I. It can be observed the hardness and elastic modulus of these composites increase with increasing MWCNTs content up to 0.1%. Beyond this value, as it can be noted from Figure 8a, an increase in MWCNTs content yields a considerable decrease of the hardness.
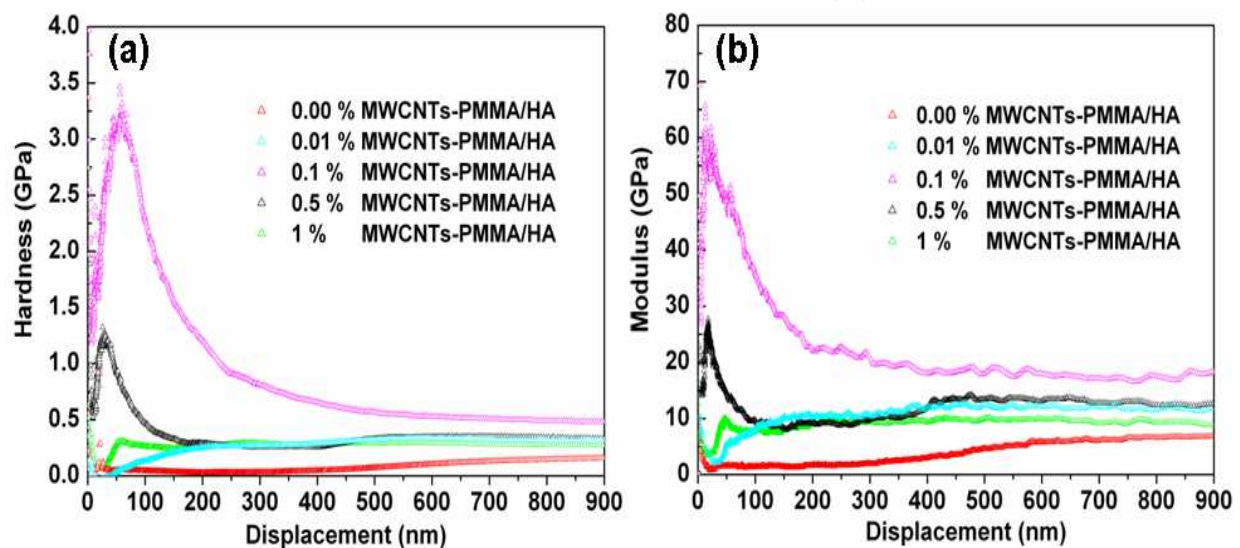

Figure 10. Hardness (a) and elastic modulus values (b) as a function of the indentation depth.

	0.00% MWCNTs- PMMA/HA	0.01% MWCNTs- PMMA/HA	0.1% MWCNTs- PMMA/HA	0.5% MWCNTs- PMMA/HA	1% MWCNTs- PMMA/HA
H (GPa)	0.288	0.510	3.460	1.321	0.624
E (GPa)	5.949	14.022	69.528	28.08	10.56

Table 1. Average values of hardness and elastic modulus for different concentrations of MWCNTs in the PMMA/HA composite.

In a previous publication (Shokuhfar et al., 2007), the authors demonstrated that there are several key requirements for an optimal fibre-reinforced, polymer-based, composite system, namely: (a) The fibres should be long enough so that the stress developed within them is significantly larger than the nominal stress on the composite; (b) The cross-sectional area of the fibre should be as small as possible - the strength of the fibre is inversely proportional to the square root of its maximum flaw size; therefore for smaller cross-sectional areas the appearance of flaws is reduced; (c) The spatial arrangement of the fibres in the matrix has to be of a significant order to ensure a unidirectional, maximal reinforcement. Also self-consistent calculations lead to the

conclusion that an isotropic arrangement of the fibres will result in the dilution of the reinforcement effect within the polymer matrix. Previously, the law of volumetric mixtures was used to analyse the mechanical behaviour of a continuous media of PMMA/HA with a blend of carbon nanotubes distributed in the matrix. According to the numerical calculations (Shokuhfar et al., 2007) carried out the Young Modulus of the composite increases with increasing MWCNTs concentration up to a concentration around 10 %. The present experimental results show that after a concentration of MWCNTs of 0.1 % a noticeable decrease of the Young Modulus is clearly identified (Figure 10b). This discrepancy may be due to the fact the modelling did not take into account two physical phenomena, which, in view of the experiments, are important, namely: 1) the interaction between nanotubes and 2) the character of the interface between the MWCNTs and the matrix. Increasing the MWCNT's concentration up to a certain level promotes a mutual interaction between a crossed pair and a coarse mesh of nanotubes (Figure 11).
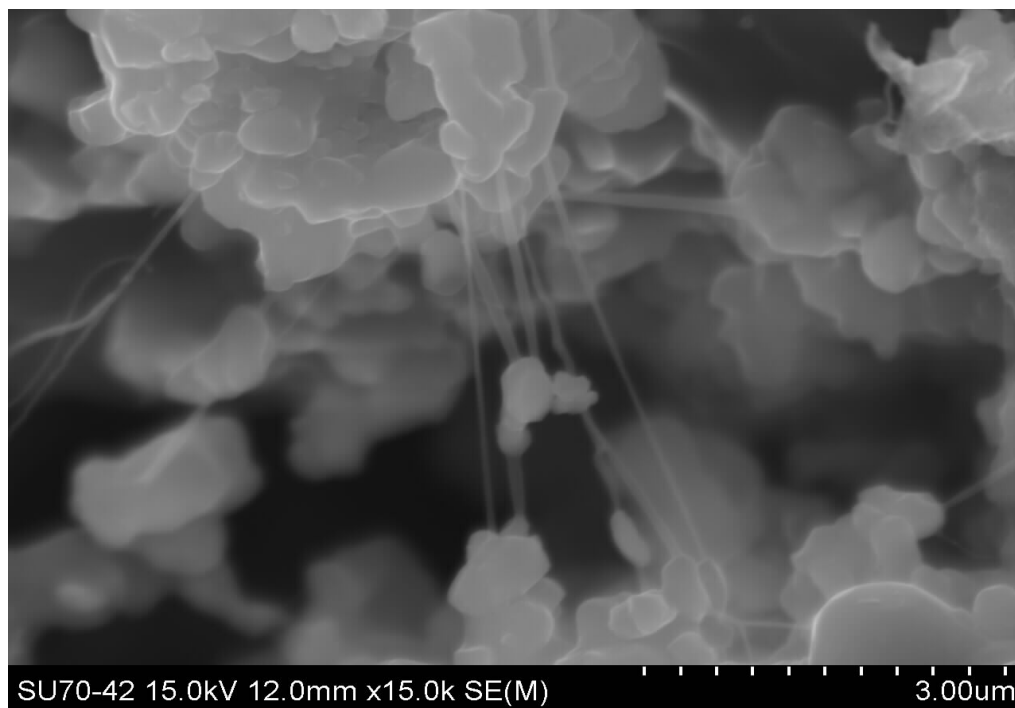

SU70-42 15.0kV 12.0mm x15.0k SE(M)   3.00um

Figure 11. FE-SEM image showing mutual interactions between crossed pair of nanotubes.

Consequently, the set of nanotubes can act as a deformation lock, either in extensional or shear mode, giving rise to improved mechanical properties. An identical behaviour was noticed by analysing the effect of the MWCNTs concentration on a PMMA matrix (Akiskalos, 2004). It should be mentioned the SEM images clearly show that after a concentration of 0.1% for the MWCNTs, a drop of homogeneity in the nanotubes-matrix contact occurs, giving rise to the formation of voids and internal cavities with the eventual reduction in the mechanical performance of the composite. In fact, most likely, these defects act as nucleation for internal crack tips and mutual link-up modes, with a fast degradation of the structure integrity and eventual breakdown. Fatigue tests were performed in artificial bones to confirm this analysis (Figure 12). In the tests, after one million of cycles the nanocomposite with 0.1% of MWCNTs-PMMA/HA does not present any signal of crack propagation and delamination (Figures 12

a,b). But when we performed the same type of fatigue tests for only PMMA nanocomposite we can clearly observed the delamination and cracks in Figures 12c and d, respectively.
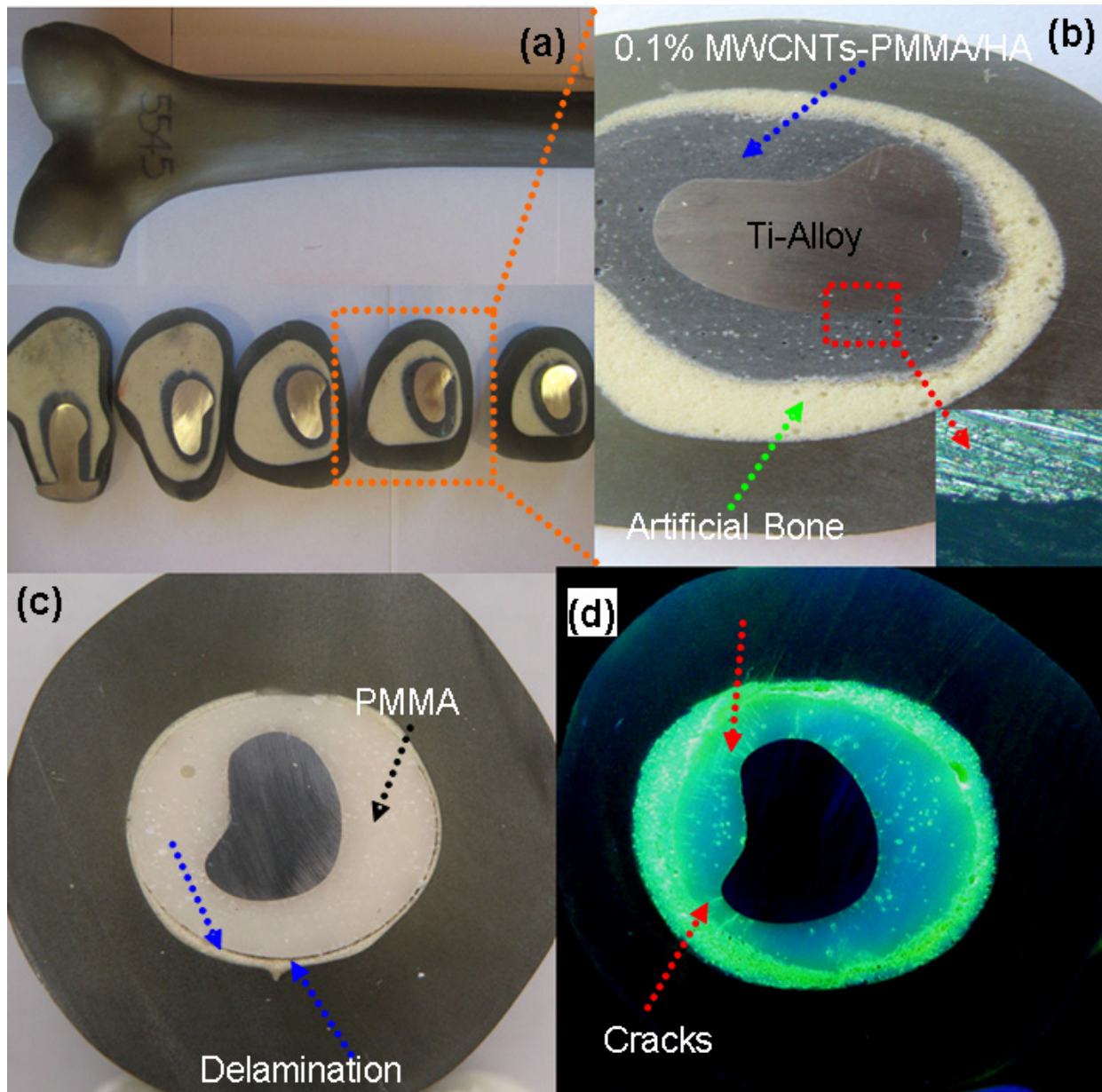

Figure 12. (a,b) Optical microscopic observation of the 0.1% MWCNTs-PMMA/HA nanocomposite at the interface with titanium prosthesis after a fatigue test for one million of cycles. (c,d) Optical microscopic image shows delamination and cracks after same type of fatigue test for only PMMA nanocomposite.

6. *In Vivo* studies of carbon nanotube-based nanocomposites

6.1. *In Vivo* methods

Animal Model: Following the experimental protocol approved by the National Ethics Committee for Laboratory Animals (Portugal) (Dias et al., 2008), two healthy, adult male

sheep with average weight of 45 kg, were used for the *in-vivo* implantation. The sheep were permanently housed indoors in group housing and were kept under a constant photoperiod cycle (light: from 07:00 to 19:00 hours; dark: from 07:00 to 19:00 hours), temperature (20 ± 2 °C) and humidity (50 ± 10%). Food was withdrawn 36 hours, and water 6 hours prior to anaesthesia.

Anesthetic and Surgical Method: Surgery was performed under general anaesthesia, which was induced with pentobarbital through intravenous injection; the animals had been previously premedicated with xilazine and buprenorphine. The anaesthesia was maintained through using isoflurane administered with an endotracheal tube and spontaneous ventilation. An electrocardiogram (ECG) monitor and a pulsioximeter were used to monitor the condition of the animals. The antibiotherapy was initiated during surgery with amoxicillin (Clamoxyl) and these therapies were maintained for one week. The site of the surgery was prepped with a solution of Betadine (povidone-iodine) and alcohol (Dura-Prep; 3M Health Care, St. Paul, MN) after the animals were locally shaved. For the implantation of the bioactive bone cement in the tibia, the animals were placed in a dorsal recumbency position and a longitudinal incision was made on the frontal surface of the left and right tibia. After exposure of the tibial bone, the periosteum was reflected and a 2.5 mm diameter pilot hole was made with a surgical drill and then enlarged with low speed drilling to a 3.0 mm diameter. During the process, the bone was continuously perfused with a sterile saline solution. Three holes were drilled on each tibia as shown in Fig. 13a and then the holes were filled with the bioactive bone cement paste (Fig. 13b). The surgery field was covered with subcutaneous tissue and the skin was closed using absorbable Surgicryl ® 2–0 sutures.

An *in vivo* paste was prepared by thoroughly mixing a monomer solution of bioactive bone cement (Johnson and Johnson Co.) with our dry powder containing the COOH-MWCNTs-reinforced PMMA/HA nanocomposite. These components were mixed together just before the *in vivo* procedure; the resultant mixture was used as a viscous paste. This biocomposite was implanted into a sheep model system, in a similar manner to previous protocols (Dias et al., 2008; Henriksen et al., 2009). For the implantation, three holes were drilled in each tibia (Figure 13a) and then the holes were filled with the bioactive bone cement paste (Figure 13b). The field of the surgical procedure was covered with subcutaneous tissue, and the skin was closed using absorbable sutures. Post-operative X-ray tests were conducted to ensure that proper filling of the holes in the bone had occurred (Fig. 14i). Twelve weeks after implantation, the animals were sacrificed following the experimental protocol approved by the National Ethics Committee for Laboratory Animals (Portugal). The implanted material and the surrounding tissue were removed.

Radiological and Histological Studies: Post-operative X-ray tests were performed with a Mammodiagnost UC system (Philips) with 28 kV, 25 mA, using coarse focus and Kodak Min-R Screen film. Twelve weeks after implantation, the animals were sacrificed with an intravenous dose of sodium pentobarbital (Eutasil®). The implanted materials and the

surrounding tissue was removed The bone specimens for the histological evaluation were fixed in 4% buffered formaldehyde, dehydrated in graded alcohols and embedded in methyl methacrylate (Merck Supplier Part: 8.00590.1000). After polymerization, non-decalcified 30 μm sections were obtained in the transversal direction using a saw microtome (Leica 1600) and then ground with silicon carbide powder. Thin sections were prepared of each specimen for evaluation by light microscopy (Eclipse 600, Nikon Japan). The bone sections were stained with toluidine blue (Brancroft and Stevens, 1996; Schipper et al., 2008).
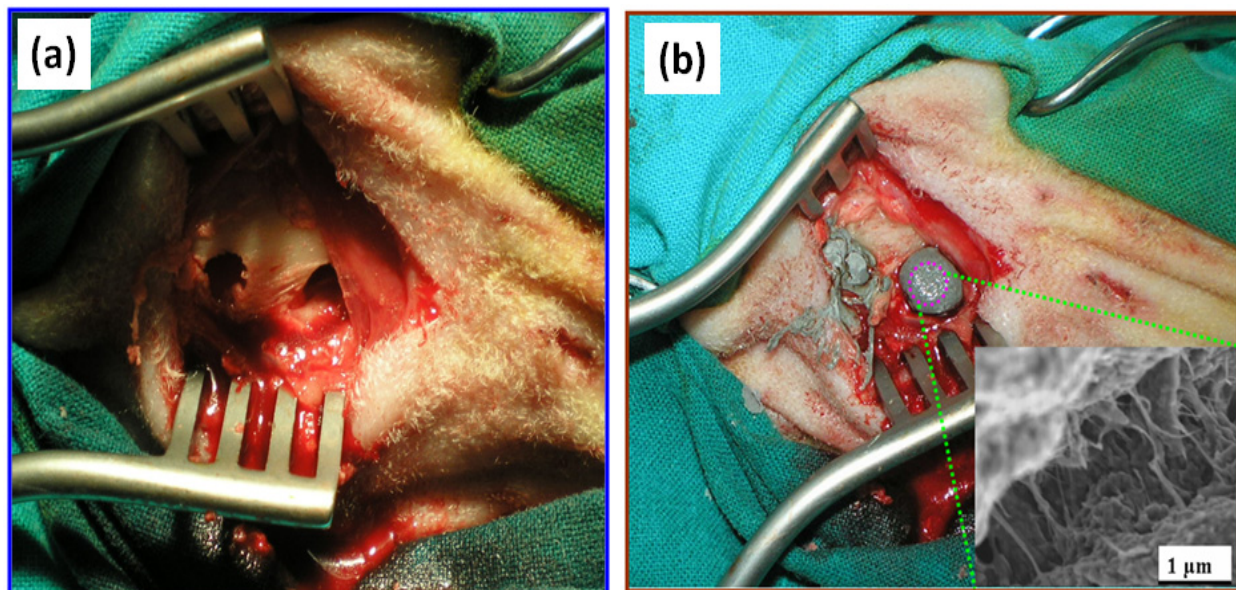

Figure 13. (a) Optical image of three holes drilled in tibial bone of a sheep before implantation (b) Digital image of filling the bone during the surgical procedure with the bioactive bone cement paste in three holes of a sheep tibia.

To examine the *in vivo* response with the nanocomposites, x-ray tests were performed. After twelve weeks the inflammatory reactions in the surrounding tissues were examined. X-rays of the left tibia were captured immediately after surgery (Fig. 14i) and then after 12 weeks (Fig. 14ii). The drilled cavities, as indicated by an asterisk in Figures 14(i) and (ii), had been invaded by the marrow region. Also, there were no signs of periosteal or bone negative reactions twelve weeks after implantation. Figures 14(iii-vi) provided a histological evaluation of the stained specimens obtained twelve weeks after implantation. The periosteum covering the outer surface of the implant and the cortical bone at the interface did not show any adverse reaction to the implants (Fig. 14iii,iv). Furthermore, the contact between the cement and the bone showed no fibrous tissues or inflammatory cells as observed in Figure 14(iii). Osteocytes (denoted by red dotted circle in Fig. 14iii) were clearly observed. At higher magnifications, a favourable interface between bone and the cement was observed (Fig. 14iv). However, in the areas where there was no direct contact between
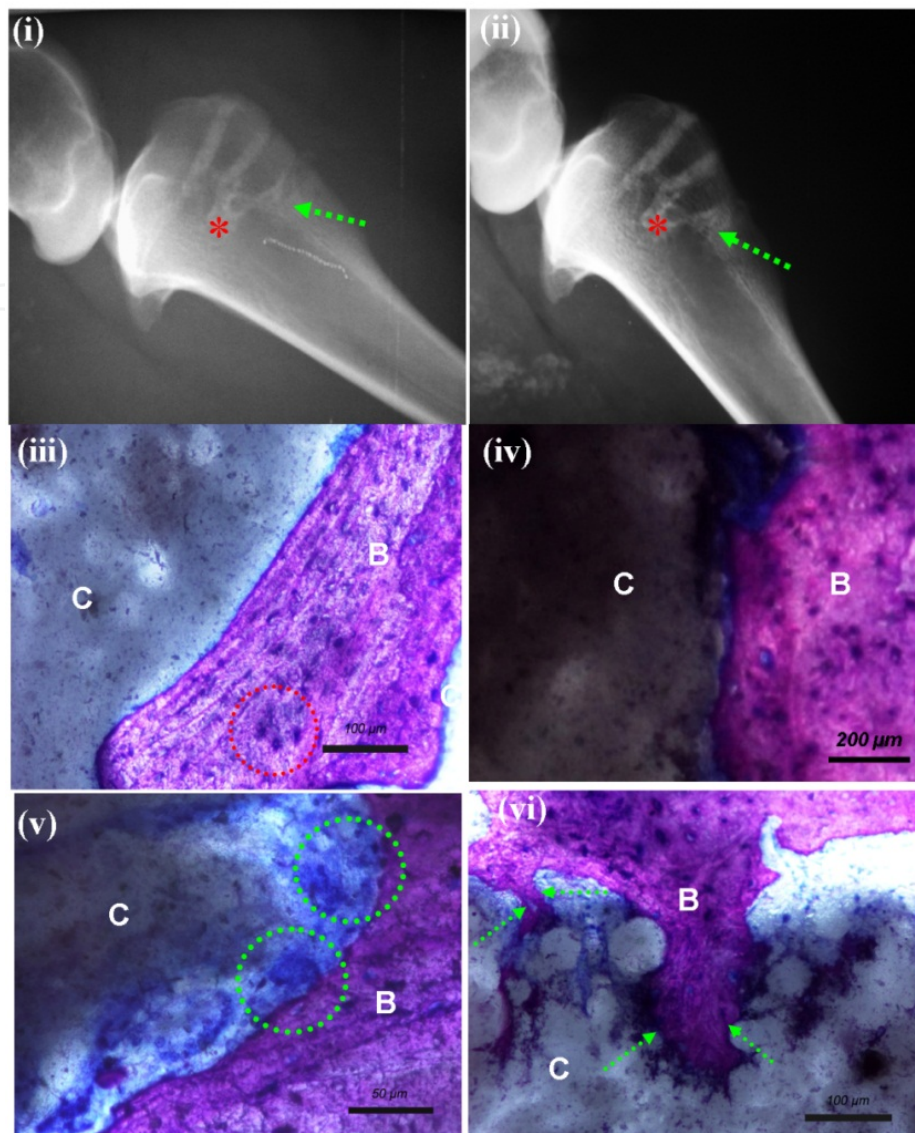
Figure 14. *In-vivo* response with the nanocomposite bone cement in sheep. (i) X-rays (left tibia) immediately after surgery and (ii) after 12 weeks. Invasion of the marrow region (indicated by the asterisk) and restoration of the cavities is observed. There are no inflammatory reactions in the surrounding tissues after 12 weeks. (iii) An image of Giemsa surface staining of the specimens at 12 weeks after implantation shows excellent contact between the nanocomposite PMMA-HA-CNT bioactive-bone cement (C) and the bone tissue (B) with no fibrous tissues and no inflammatory cell infiltration. Oteocytes, which are indicated by the red dotted circle regions, are observed (iv) An image of Giemsa surface staining focusing on the interface between the nanocomposite bioactive-bone cement and the tissue (C) and the bone tissue (B), which is very favourable. (v) An image of Giemsa surface staining focusing revealing multinuclear osteoclast-like cells covering the surface of the bone cement, as indicated by the green dotted circles; there was no direct contact between bioactive-bone cement (C) and bone tissue (B) generally observed. (vi) An image of Giemsa surface staining focusing showing that the new bone (B) clearly enters into the pores of the bone cement (C), as indicated by the green dotted arrow.

the bone and the implant, osteoclast-like-cell (Yavropoulou and Yovos, 2008) appeared on the cement surface (indicated by the green dotted circle in Fig. 14v). Furthermore, in our specimens (Fig. 14vi), new bone (B) clearly penetrated the pores of the bone cement (C), as

indicated by the green dotted arrow. The biocompatibility and osteoconductivity are critical factors as foreign material reside *in-vivo*. A post-mortem examination of the tibias revealed that the implants were completely covered by the periosteum. This finding was determined by fixing the regional lymph nodes with 4% formaldehyde, embedding them in paraphin, and then cutting them into 30 μm sections with a microtome (Leica, Jung RM 2045). The specimens were stained with hematoxylin/eosin to examine the biocompatibility and osteoconductivity responses. The histological response of the regional lymph nodes revealed no significant morphologic changes in the regional lymph nodes between the control and test groups. The histological evaluations demonstrate that the CNT-reinforced composite with the bioactive-bone cement responded favourably as a tibial bone implant based on its osteoconductivity and biocompatibility results. This biocompatibility has been demonstrated for an extended time period of 12 week post-operation for our 0.1% MWCNTs-PMMA/HAp nanocomposites.

7. Conclusions

Herein, we demonstrate a *freeze-granulation technique* to synthesis a novel nanocomposite of carbon nanotube reinforced PMMA/HA for next generation biomedical applications. By using this method it is possible to increase material homogeneity and also optimize the % of MWCNTs in the PMMA/HA matrix. We shows that the concentration of 0.1% of MWCNTs performs the best reinforcement for the PMMA/HA nanocomposites. The hardness and elastic modulus of MWCNTs-reinforced PMMA/HA nanocomposites increase with the increasing concentration of nanotubes up to around 0.1% in weight. Beyond this limit, further addition of MWCNTs in PMMA/HA matrix yields a considerable decrease of these mechanical properties. This can be explained in terms of the nanotube-matrix contact homogeneity – a further increase of the nanotubes may lead to the formation of voids and internal cavities, which can negatively impact the mechanical performance of the composite.

In addition to this, we have found that the use of COOH-functionalized MWCNTs reinforced with PMMA/HA will provide tremendous advancements in the field of regenerative medicine. Of singular importance is the mechano-physical advantage this nanocomposite, which provides for bearing mechanical loads and promoting osteointegration with surrounding bone tissues. These are features not observed with previous materials. Our *in vivo* animal studies shows, new bone extended into the bioactive bone cement. These results confirm that this novel bionanocomposite will be an excellent candidate for bone integration due to its osteoconductivity and biocompatibility. We believe that these results will have applications in a diversity of areas including nanotechnology, biomaterials, and regenerative medicine.

Author details

Manoj Kumar Singh*, L. Syam Sundar, Ranjit Hawaldar, Elby Titus, Jose Gracio
Centre for Mechanical Technology and Automation (TEMA), University of Aveiro, 3810-193 Aveiro, Portugal

---

* Corresponding Author

Acknowledgement

8. References

D.E. Discher, P. Janmey, Y. Wang, Tissue Cells Feel and Respond to the Stiffness of Their Substrate, Science, 2005, 310, 1139-1143.

P.R. LeDuc, D.R. Robinson, Using lessons from cellular and molecular structures for future materials, Adv. Mater., 2007, 19(22), 3761–3770.

P.R. LeDuc, R.R. Bellin, Nanoscale intracellular organization and functional architecture mediating cellular behaviour, Ann. Biomed Eng., 2006, 34 (1), 102-13.

L.P. Zanello, B. Zhao, H. Hu, R.C. Haddon, Bone cell proliferation on carbon nanotubes, Nano Letters, 2006, 6, 562.

C.-W. Lam, J.T. James, R. McCluskey, R.L. Hunter, ulmonary toxicity of single-wall carbon nanotubes in mice 7 and 90 days after intratracheal instillation, Toxicological Sciences, 2004, 77, 126.

V.L. Colvin, The potential environmental impact of engineered nanomaterials, Nat. Biotechnology, 2003, 21, 1166-1170.

P.M. Ajayan, J.M. Tour, Nanotube composites, Nature, 2007, 447, 1066-1068.

J.N. Coleman, U. Khan, Y.K. Gun'ko, Mechanical Reinforcement of Polymers Using Carbon Nanotubes, Adv. Mater., 2006, 18, 689–706.

P. Rimessi, P. Sabatelli, M. Fabris, P. Braghetta, E. Bassi, P. Spitali, G. Vattemi, G. Tomelleri, L. Mari, D. Perrone, A. Medici, M. Neri, M. Bovolenta, E. Martoni, N.M. Maraldi, F. Gualandi, L. Merlini, M. Ballestri, L. Tondelli, K. Sparnacci, P. Bonaldo, A. Caputo, M. Laus, A. Ferlini, Cationic PMMA Nanoparticles Bind and Deliver Antisense Oligoribonucleotides Allowing Restoration of Dystrophin Expression in the mdx Mouse, Molecular Therapy, 2009, 175, 820-827.

M.K. Singh, T. Shokuhfar, J. Gracio, A.C.M. Sousa, J. Fereira, H. Garmestani, S. Ahzi, Hydroxyapatite Modified with Carbon-Nanotube-Reinforced Poly(methyl methacrylate): A Nanocomposite Material for Biomedical Applications, Adv. Funct. Mater., 2008, 18, 694-700.

W.A. Curtin, B.W. Sheldon, CNT-reinforced ceramics and metals, Mater. Today, 2004, 7, 44.

C.I. Vallo, G.A. Abraham, T.R. Cuadrado, J.S. Roman, Influence of cross-linked PMMA beads on the mechanical behavior of self-curing acrylic cements, J. Biomed Mater Res. B, 2004, 70, 407-416.

M.A. McGee, D.W. Howie, K. Costi, D.R. Haynes, C.I. Wildenauer, M.J. Pearcy, J.D. McLean, Implant retrieval studies of the wear and loosening of prosthetic joints: a review, Wear, 2000, 241, 158-165.

M.M. Stevens, Biomaterials for bone tissue engineering, Mater. Today 2008, 11, 18-25.

H. Dai, Carbon nanotubes: opportunities and challenges, Surf Sci., 2002, 500, 218.

Min-Feng Yu, Oleg Lourie, Mark J. Dyer, Katerina Moloni, Thomas F. Kelly, Rodney S. Ruoff, Strength and Breaking Mechanism of Multiwalled Carbon Nanotubes Under Tensile Load, Science, 2000, 287 (5453) 637–640.

Bei Peng, Mark Locascio, Peter Zapol, Shuyou Li, Steven L. Mielke, George C. Schatz, Horacio D. Espinosa, Measurements of near-ultimate strength for multiwalled carbon nanotubes and irradiation-induced crosslinking improvements, Nature Nanotechnology, 2008, 3 (10) 626–631.

P.G. Collins, They are stronger than steel, but the most important uses for these threadlike macromolecules may be in faster, more efficient and more durable electronic devices, Scientific American, 2000, 67–69.

M. Popov, Superhard phase composed of single-wall carbon nanotubes, Physical Review B, 2003, 65 (3), 033408.

Y. Ying, R. K. Saini, F. Liang, A. K. Sadana and W. E. Billups, Functionalization of Carbon Nanotubes by Free Radicals, Org. Lett., 2003, 5, 1471.

C. A. Dyke, J. M. Tour, Solvent-Free Functionalization of Carbon Nanotubes, J. Am. Chem. Soc., 2003, 125, 1156.

V. Georgakilas, D. Voulgaris, E. Vazquez, M. Prato, D. M. Guldi, A. Kukovecz, H. Kuzmany, Purification of HiPCO Carbon Nanotubes via Organic Functionalization, J. Am. Chem. Soc., 2002, 124, 14318.

C. A. Dyke, J. M. Tour, Overcoming the Insolubility of Carbon Nanotubes Through High Degrees of Sidewall Functionalization, Chem. Eur. J., 2004, 10, 812.

T. Wang, C. Tseng, Polymeric carbon nanocomposites from multiwalled carbon nanotubes functionalized with segmented polyurethane, Journal of Applied Polymer Science, 2007, 105, 1642.

Y. Zho, F. Stoddart, Noncovalent Functionalization of Single-Walled Carbon Nanotubes. Accounts of Chemical Research, 2009, 42 (8), 1161-1171

S. C. Tsang, Y. K. Chen, P. J. F. Harris, M. L. H. Green, A simple chemical method of opening and filling carbon nanotubes, Nature, 1994, 372, 159.

S. Iijima, Helical microtubules of graphitic carbon, Nature, 1991, 354, 56.

R. H. Baughman, A. A. Zakhidov, W. A. de Heer, Carbon Nanotubes--the Route Toward Applications, Science, 2002, 787, 297.

Y. Usui, Y.K. Aoki, N. Narita, N. Murakami, I. Nakamura, K. Nakamura, N. Ishigaki, H. Yamazaki, H. Horiuchi, H. Kato, S. Taruta, Y.A. Kim, M. Endo, N. Saito, Carbon Nanotubes with High Bone-Tissue Compatibility and Bone-Formation Acceleration Effects. Small, 2008, 4, 240.

G. Goller, H. Demirkiran, F. N. Oktar, E. Demirkesen, Processing and characterization of bioglass reinforced hydroxyapatite composites, Ceram. Int., 2003, 29, 721

J. Cholpek, B. Czajkowska, B. Szaraniec, F. Beguin, In vitro studies of carbon nanotubes biocompatibility, Carbon, 2006, 44, 1106.

R. L. Price, M. C. Waid, K. M. Haberstroh, T. J. Webster, Selective bone cell adhesion on formulations containing carbon nanofibers, Biomaterials, 2003, 24, 1877

A. Peigney, Composite materials: Tougher ceramics with nanotubes, Nat. Mater., 2003, 2, 15.

S. Dimitrievska, J. Whitfield, S.A. Hacking, M.N. Bureau, Novel carbon fiber composite for hip replacement with improved in vitro and in vivo osseointegration. J Biomed Mater Res A, 2008, 91 (1) 37-51

A. A. White, S. M. Best, Hydroxyapatite–carbon nanotube composites for biomedical applications: a review, Int. J. Appl. Ceram. Technol., 2007, 4, 1.

A. Kis, G. Csanyi, J. -P. Salvetat, T. -N. Lee, E. Couteau, A. J. Kulik, W. Benoit, J. Brugger, L. Forro, Reinforcement of single-walled carbon nanotube bundles by intertube bridging, Nat. Mater., 2004, 3, 153.

B. C. Satishkumar, A. Govindaraj, J. Mofokeng, G. N. Subbanna, C. N. R. Rao, Novel experiments with carbon nanotubes: opening, filling, closing and functionalizing nanotubes, J. Phys. B, 1996, 29, 4925.

S. C. Tsang, Y. K. Chen, P. J. F. Harris, M. L. H. Green, Nature, 1994, 372, 159.

Y. Chen, C. H. Gan, T. H. Zhang, G. Yu, P. Bai and A. Kaplan, Laser-surface-alloyed carbon nanotubes reinforced hydroxyapatite composite coatings, Appl. Phys. Lett., 2005, 86, 251905.

A. M. Walker, Y. Tao, J. M. Torkelson, Polyethylene/starch blends with enhanced oxygen barrier and mechanical properties: Effect of granule morphology damage by solid-state shear pulverization, Polymer, 2007, 48, 1066.

N. Poudyal, B. Altuncevahir, V. Chakka, K. Chen, T. D. Black, J. Liu, Y. Ding, Z. L. Wang, Field-ball milling induced anisotropy in magnetic particles , J. Phys. D: Appl. Phys., 2004, 37, L45.

S. Haque, I. Rehman, J. A. Darr, Synthesis and characterization of grafted nanohydroxyapatites using functionalized surface agents, Langmuir 2007, 23, 6671.

E. Bouyer, F. Gitzhofer, M. I. Boulos, Journal of Materials Science: Materials in Medicine, 2000, 11, 523.

P. Meneghetti, S. Quantubuddin, S. Webber, Synthesis of polymer gel electrolyte with high molecular weight poly(methyl methacrylate)–clay nanocomposite, Electrochim Acta, 2004, 49, 4923

J. G. Ryu, S. W. Park, H. Kim, J. W. Lee, Power ultrasound effects for in situ compatibilization of polymer-clay nanocomposites, Materials Science and Engineering C, 2004, 24, 285.

C. Velasco-Santos, A. L. Martínez-Hernández, F. T. Fisher, R. Ruoff, V. M. Castaño, Improvement of Thermal and Mechanical Properties of Carbon Nanotube Composites through Chemical Functionalization, Chem. Mater., 2003, 15, 4470.

C. Velasco-Santos, A. L. Martìnez-Hernández, M. Lozada-Cassou, A. Alvarez-Castillo, V. M. Castańo, Chemical functionalization of carbon nanotubes through an organosilane, Nanotechnology, 2002, 13, 495.

P. P. Hong, F. J. Boerio, S. D. Smith, Surface segregation in blends of polystyrene and deuterated polystyrene, Macromolecules, 2002, 35, 5140.

M. Paillet, V. Jourdain, P. Poncharal J. Sauvajol, J. C. Meyer, B. Chaudret, Versatile Synthesis of Individual Single-Walled Carbon Nanotubes from Nickel Nanoparticles for the Study of Their Physical Properties, J. Phys. Chem. B, 2004, 108, 17112.

F. F. M. de Mul, M. H. J. Hottenhuis, P. Bouter, J. Greve, J. Arends, J. J. Ten Bosch, Micro-Raman line broadening in synthetic carbonated hydroxyapatite, J. Dent Res., 1986, 65, 437.

M. Suzuki, H. Kato, S. Wakumoto, Vibrational Analysis by Raman Spectroscopy of the Interface Between Dental Adhesive Resin and Dentin, J. Dent Res., 1991, 70, 1092.

S.B. Kim, Y.J. Kim, T.L. Yoon, S.A. Park, I.H. Cho, J.K. Eun, I.A. Kim, J. Shin, The characteristics of a hydroxyapatite-chitosan-PMMA bone cement. Biomaterials, 2004, 25, 5715-5723.

A. Matsushita, Y. Ren, K. Matsukawa, H. Inoue, Y. Minami, I. Noda, Y. Ozaki, Two-dimensional Fourier-transform Raman and near-infrared correlation spectroscopy studies of poly (methyl methacrylate) blends: 1. Immiscible blends of poly(methyl methacrylate) and atactic polystyrene, Vibrational Spectroscopy, 2000, 24, 171.

X. Li, B. Bhushan, A review of nanoindentation continuous stiffness measurement technique and its applications, Mater. Charact. 2002, 48, 11.

B. Bhushan, X. Li, Nanotribology and nanomechanics in nano/biotechnology, Int. Mater. Rev. 2003, 48, 125.

T. Shokuhfar, E. Titus, G. Cabral, A. C. M. Sousa, J. Gracio, W. Ahmed, T. I. T. Okpalugo, A. Makradi, S. Ahzi, On the mechanical properties of nanocomposite hydroxypatite (HA)/PMMA/CNT , International Journal of Nanomanufacturing, vol. 1, no. 2, pp. 107-115, 2007

T. Shokuhfar, A. Makradi, E. Titus, G. Cabral, S. Ahzi, A. C. M. Sousa, S. Belouettar, J. Gracio, Hydroxyapatite Modified with Carbon-Nanotube-Reinforced Poly(methyl methacrylate): A Nanocomposite Material for Biomedical Applications, Journal of Nanoscience and Nanotechnology 2007 in press.

T. Akiskalos, MSc Thesis, Department of Mechanical Engineering, Massachusetts Institute of Technology (MIT) 2004.

I.R. Dias, C.A. Viagas, J.T. Azevedo, E.M. Costa, P. Lourenco, A. Rodrigues, A.S. Cabrita, Assessment of markers of bone formation under controlled environmental factors and their correlation with serum minerals in adult sheep as a model for orthopaedic research, Laboratory Animals, 2008, 42, 465-472.

K. Henriksen, A.V. Neutzsky-Wulff, L.F. Bonewald, M.A. Karsdal, Local communication on and within bone controls bone remodeling, Bone, 2009, 44, 1026-1033.

J.D. Brancroft, A. Stevens, Theory and practice of histological techniques, Edinburgh: Churchill Livingstone, 1996, 99-211.

M.L. Schipper, N. Nakayama-Ratchford, C.R. Davis, N.W.S. Kam, P. Chu, Z. Liu, X. Sun, H. Dai, S.S. Gambhir, A pilot toxicology study of single-walled carbon nanotubes in a small sample of mice., Nature Nanotechnology, 2008, 3, 216-221.

M.P. Yavropoulou, J.G. Yovos, Osteoclastogenesis-Current knowledge and future perspectives, J. Musculoskelet Neuron